Central-axis depth-dose data for diagnostic radiology

1981 Phys. Med. Biol. 26 657

(http://iopscience.iop.org/0031-9155/26/4/009)

Phys. Med. Biol., 1981, Vol. 26. No. 4, 657–670. Printed in Great Britain

Central-axis depth–dose data for diagnostic radiology

R M Harrison

Regional Medical Physics Department, Newcastle General Hospital, Newcastle upon Tyne NE4 6BE, England

Received 29 August 1980, in final form 27 November 1980

Abstract. Depth–dose data have been measured for a range of irradiation conditions relevant to diagnostic radiology in order to provide a basis for the calculation of patient dosage arising from X-ray examinations. In general, data are required for larger field sizes, longer source–surface distances and greater tube filtrations than are commonly encountered in radiotherapy. Principles and techniques of measurement are discussed with particular attention to the specification of X-ray beam quality. It is recommended that both peak tube potential and first half-value thickness should be specified, especially for the determination of doses at depths of 5 cm or more. With the appropriate specification of quality, good agreement is found between these measurements and other compilations of depth–dose data for radiotherapy use. Zero-area depth–doses have also been measured and compared with calculated values derived from theoretical considerations of X-ray beam spectra.

1. Introduction

The determination of patient dosage in diagnostic radiology is important if radiation doses are to be minimised whilst satisfactory image quality is still maintained. Although it is accepted that a complete description of internal dose distributions must allow for the differing absorption coefficients of the component tissues, the first stage in the calculation of the dose within a patient requires a knowledge of central-axis depth–dose data in a standard material (water) in the appropriate quality range. These data may then be used in a manner directly analogous to the long-established methods of radiotherapy dosimetry.

As in radiotherapy, calculations based on such data require a knowledge of certain irradiation parameters (e.g. tube potential, tube current, X-ray output, source–surface distance (SSD), filtration, field size and exposure time) and may be supplemented by direct measurements of skin doses using, for example, thermoluminescence dosimetry (TLD).

Although depth–dose data in the relevant quality range (1–4 mm Al half-value thickness (HVT)) are available for radiotherapy purposes (e.g. *Br. J. Radiol. Suppl.* 11 1972) they must be applied to diagnostic examinations with caution, since they refer, in general, to shorter SSDs and smaller field sizes than are commonly encountered in diagnostic radiology. Also, primary beam filtration for radiotherapy use is often considerably less than is desirable for diagnosis for which minimum filtration values are recommended by the *Code of Practice for Protection of Persons against Ionizing Radiations arising from Medical and Dental use* (1972).

This paper reports measurements of central-axis depth–doses for a range of field sizes and X-ray beam qualities corresponding to the irradiation conditions encountered in diagnostic radiology where X-ray tubes with tungsten targets are employed.

The practical estimation of patient dosage at any point on the central axis of the beam requires a separate measurement of the surface dose (e.g. using TLD) if only percentage depth–dose (PDD) data are available. If surface doses are not known or cannot easily be measured, backscatter factors (BSF) for the appropriate beam qualities and field sizes are required which enable surface doses to be calculated from a measurement of the exposure at a point in air on the central axis. It may be convenient to express depth–dose data in the form of tissue–air ratios (TARs) for this purpose. This technique has the advantage that dose calculations can be made from a knowledge of the properties of the X-ray beam as in radiotherapy, without the need for individual patient measurements, which are both time consuming and inappropriate where large numbers of patients are involved. Furthermore, this method enables dose estimates to be made retrospectively.

For practical purposes, BSFs given in *Br. J. Radiol. Suppl.* 11 (1972) may be used together with the PDD data presented in this paper without serious error. However, since these BSFs are quoted as a function only of the first HVT which alone does not completely specify beam quality in the diagnostic range, further experimental work on BSFs is in progress and will be submitted for separate publication.

2. General experimental principles

2.1. Specification of beam quality

The usual starting point for the specification of beam quality is the first HVT although it has long been appreciated that this parameter alone may be inadequate (Greening 1963). The additional specification of the peak tube potential (kV_p) and the second HVT (or homogeneity coefficient, i.e. the ratio of first to second HVT) provide further information, which may be sufficient for most practical purposes, though a complete specification would require a knowledge of the entire X-ray spectrum.

It may be expected, therefore, that for a particular first HVT (assuming fixed field size and SSD) the percentage depth–dose at a given depth will not be uniquely defined, since a combination of high peak tube potential and low filtration may be chosen to give the same first HVT as a combination of lower tube potential and higher filtration. As an example, a first HVT of 2 mm Al may be obtained with 100 kV_p and 1.1 mm Al total filtration, or 50 kV_p and 2.8 mm Al total filtration (HPA 1977, figure B3). At a depth of, say, 10 cm the percentage depth–dose for the latter combination will be less than that for the former.

The comprehensive documentation of depth–dose data in the range 1–4 mm Al HVT given in *Br. J. Radiol. Suppl.* 11 (BJR 1972) was intended for radiotherapy applications where superficial regions of the body are of most interest. Consequently, the first HVT is a reasonable guide to beam quality for these purposes. For diagnostic applications, however, it may be necessary to know the doses at depths up to, say, 20 cm, corresponding to four or more HVTs.

In this paper beam quality is specified by the first HVT together with the peak tube potential. Depth–dose measurements maɑe for a number of values of peak tube potential for each value of the first HVT confirm the appropriateness of this quality specification.

2.2. Zero-area depth–dose data

Although relatively large field sizes are commonly encountered in radiology, it is important to include measurements of zero-area data so that the scatter contribution at a point may be estimated by subtraction of the zero-area dose from the total depth–dose. Moreover, the primary radiation is responsible for the formation of the radiographic image whilst scattered radiation contributes significantly to patient dosage without providing any extra information.

Attenuation measurements were made using a narrow beam technique. The results represent narrow-beam depth–doses for an infinite SSD. An appropriate inverse square correction was made to convert to the SSD used for the in-phantom measurements.

Zero-area data were also determined by calculating X-ray spectra theoretically using the method of Birch and Marshall (1979). Their computer program was used and modified only by the substitution of some alternative routines for the Harwell subroutines originally used. This leads to discrepancies in the number of photons per unit energy interval of not more than ±3% between the resulting spectra used here and the original calculated spectra (Birch, private communication). The calculated spectra refer to constant tube potentials whereas measurements were made with a pulsating tube potential. Nevertheless, comparison between experiment and theory is possible for the same peak tube potential and first HVT and for this purpose a subroutine was added to the original program to calculate first and second HVTs in aluminium. For a given spectrum, the numbers of photons per unit energy interval were calculated as the simulated beam was attenuated by various depths of water. For each depth, the numbers of photons were converted into kerma-in-tissue using the conversion factors of Birch *et al* (1979) and summed over the whole spectrum to give the total kerma and hence the percentage depth–dose. The ratio of the mass–energy transfer coefficients for water and tissue varies by <4% over the diagnostic energy range, so that theoretical data for tissue may sensibly be compared to experimental data in water particularly when the "smoothing" effect of a spectrum of photon energies is considered.

2.3. Choice of detector

Two conflicting requirements of detector volume must be considered for measurements in a water phantom at diagnostic energies (20–120 keV). Because of the rapid attenuation in water of X-ray beams in this quality range (e.g. the HVT is 1.5 cm in water at 60 kV_p) the detector volume must be large enough to provide measurable ionisation at large depths without incurring anode heating problems due to long exposure times. At the same time, a chamber that displaces a large volume of water incurs several errors. If it is assumed to measure the exposure at its centre, the reading due to primary X-rays will be in error because of lack of attenuation by the air volume. Conversely, the scattered radiation from this volume is absent though this loss may be partially offset by the decreased attenuation of the scatter originating at larger distances from the detector. In addition, an exposure gradient will exist across the chamber (e.g. 3% per mm at 60 kV_p). The overall effect is difficult to predict.

For these measurements a detector volume of 0.3 cm^3 with a chamber thickness 0.15 cm constitutes an acceptable compromise. The response of the detector to a given absorbed dose should ideally be constant throughout the energy range 20–120 keV.

3. Apparatus and measurement technique

A Medio-DLX X-ray set and Machlett Dynamax tube with a 16° tungsten target, full-wave rectified waveform and nominal 2 mm focus were used for all measurements.

Depth–dose and HVT measurements were made with a 0.3 cm^3 NE 2502 soft X-ray chamber connected to an NE Ionex 2500/3 exposure meter. The chamber thickness was 0.15 cm and the point of measurement was taken to be at the mid-point of the volume.

The response per unit exposure of the chamber as a function of beam quality was determined by comparison in air with a calibrated secondary standard dosemeter over the range 1–7 mm Al HVT. The response per unit absorbed dose was then calculated using the f-factors given in ICRU 23 (1973; table 2, p 4). Although f-factors vary by around 10% over the quantum energy range 20–100 keV, f-factors corresponding to diagnostic X-ray spectra vary by <3% over the quality range 1–8 mm Al HVT. For comparison, f-factors were also calculated from the theoretical spectra of Birch *et al* (1979) using f-factors for monochromatic beams in water (ICRU 1970) and are shown in table 1. The variation in response of the chamber for a given absorbed dose was found to be 3% over the quality range 1–7 mm Al HVT.

Table 1. f-factors for some diagnostic X-ray beam spectra

Peak tube potential	60	60	100	100
First HVT (mm Al)	1.55	3.77	3.50	8.33
Total filtration (mm Al)	1.5	1.5	2.5	2.5
Attenuating medium	air	10 cm tissue	air	20 cm tissue
f-factor (from theoretical spectra and ICRU 1970)	0.88	0.89	0.90	0.92
f-factor (ICRU 1973)	0.87	0.87	0.87	0.89

The calculated f-factors apply, of course, only to the primary component of the beam, although those given in ICRU 23 (1973) make some allowance for scattered radiation. However, Epp and Weiss (1967) in a study of the spectral fluence of scattered radiation at diagnostic qualities found that the scattered component at a point in water is not much softer than the primary component at that point. In any case, the first HVTs of the total radiation contribution for the depths, field sizes and peak tube potentials used in this study are within the range over which the 3% variation in response per unit absorbed dose of the chamber is observed. Overestimates in PDD are likely to be around 3% only for the lower tube potentials ($\simeq$60 kV_p) and greater depths ($\gtrsim$10 cm water).

The tube output was always monitored using an NE Type 2561 0.3 cm^3 chamber in a corner of the X-ray field close to the collimators, in conjunction with an NE Type 2560 exposure meter and digital voltmeter.

First and second HVT measurements in aluminium were made for a range of indicated peak tube potentials and total filtrations. Aluminium absorbers were placed half way between the chamber and the X-ray focus. The X-ray beam was collimated by the field-defining diaphragm and an additional lead collimator placed at the position of the absorbers so that a 2.5 cm diameter X-ray beam was produced at the chamber. HVTs were also measured for larger field sizes. The values obtained by extrapolation to zero area (Trout *et al* 1960) indicated that the former effectively constituted narrow-beam conditions.

Peak tube potentials at all tube currents used were measured with a voltage divider and close agreement with indicated values found.

Depth–dose measurements were made in a water tank with the soft X-ray chamber encased in a 5 μm thick nylon sleeve which was later replaced by a more flexible 20 μm thick latex rubber sleeve. The chamber was moved manually along the central axis of the X-ray beam. The expected 'heel effect' was observed along the anode–cathode axis. Measurements along this axis made in air at 60 cm source–chamber distance showed that the exposure was a linear function of distance across a 14 cm wide field, so that a central-axis measurement in a water phantom will not differ appreciably from a flat-field measurement for this field size, whatever the actual value of the exposure gradient. Larger field sizes may lead to small differences in central-axis dose compared to a flat field. Measurements along the axis perpendicular to the anode–cathode axis did not vary by more than 10% across a 24 cm × 24 cm field. The mean of four values of exposure, each at a point 10.5 cm from the central axis along both axes was 90% of the central-axis value. No correction has been made to depth–dose measurements for beam non-uniformity since these data are intended primarily for diagnostic radiology applications where a 'heel effect' of some degree will always be present. For depth–dose measurements, peak tube potentials of 60, 75, 90 and 100 kV_p were employed, each value being used with 0, 0.55, 1.0 and 2.0 mm of added aluminium filtration. Measurements for each combination of peak tube potential and filtration were made at depths of 0, 1, 2, 3, 4, 6, 8, 10 and 14 cm for geometric field sizes of 7×7, 10×10, 15×15 and 30×30 cm^2 at 60 cm SSD. Selected measurements were also made at 1.14 mm Al HVT and 100 cm SSD in order to test the validity of formulae for conversion from one SSD to another (e.g. Burns 1958, and in BJR 1972 pp 101–3) at this quality. The same values of tube current and exposure time were used for the depth–dose measurements as for the HVT measurements in order to ensure that the same tube voltage waveform was used in each case. Tube currents were typically 300 mA and the voltage waveform was observed to be full-wave rectified.

Zero-area depth–dose measurements were made for the same range of HVTs and tube potentials as the large-field measurements. The attenuation of a narrow X-ray beam through various depths of water was measured using essentially the same technique as that used in the determination of HVT. The inverse square law was tested for narrow X-ray beams generated at 60 kV_p and 100 kV_p with no added filtration and found to apply, within experimental error, over the range of SSDs from 30 to 110 cm.

4. Results

Table 2 shows measured first and second HVTs and smoothed values of homogeneity coefficients for various combinations of peak tube potential and total filtration. An inherent tube filtration of 0.9 ± 0.1 mm Al was deduced from the HVT data for full-wave rectification given by the HPA (1977; figure B3).

Separate plots of percentage depth–dose were made against depth, field size and first HVT in order to produce a consistent set of data. Tables 3–7 show the depth–dose data for 1.0, 1.5, 2.0, 3.0 and 4.0 mm Al HVT and various field sizes including zero area. Extrapolation of the measured data to a depth of 16 cm has been made.

5. Errors and uncertainties

The observed precision of a single depth–dose measurement in the depth range 0 to 5 cm is less than ±1% (± standard deviation), in the range 5 to 10 cm it is less than ±3% and in the range 10 to 14 cm, less than ±6%.

Somewhat higher precision can be ascribed to be tabulated data, however, because of the averaging of readings and smoothing involved in the production of a consistent

Table 2. Smoothed first and second HVTs and homogeneity coefficients for various combinations of peak tube potential and total filtration. The inherent filtration has been taken as 0.9 mm Al.

Peak tube potential (kV_p)	Total filtration (mm Al)	First HVT	Second HVT	Homogeneity coefficient (H)
60	0.9	1.14	1.69	0.675
	1.45	1.54	2.26	0.681
	1.9	1.89	2.68	0.705
	2.9	2.29	3.06	0.748
75	0.9	1.39	2.36	0.589
	1.45	1.82	3.06	0.595
	1.9	2.22	3.48	0.638
	2.9	2.72	3.88	0.701
90	0.9	1.67	3.01	0.555
	1.45	2.17	3.85	0.564
	1.9	2.63	4.32	0.609
	2.9	3.25	4.73	0.687
100	0.9	1.96	3.64	0.538
	1.45	2.55	4.60	0.554
	1.9	3.10	5.16	0.601
	2.9	3.79	5.59	0.678

set of data. The increasing uncertainty with depth is due to the measurement of small ionisation currents at the greater depths.

In addition, uncertainties exist in the measurement of depth, field size, peak tube potential and HVT, and can be represented by standard deviations σ_d, σ_a, σ_{kV} and σ_{HVT} respectively. The assumption, for example, that $\sigma_d = 0.1$ cm, $\sigma_{kV} = 2$ kV, $\sigma_{HVT} = 0.02$ mm Al and σ_a is negligible, yields a percentage standard deviation of about 5% in percentage depth–dose for all depths at 60 kV_p and about 2% for all depths at 100 kV_p.

6. Discussion of results

An indication of the inadequacy of the first HVT as the sole specifier of beam quality at depths of several centimetres is given in figure 1 which is a graph of percentage depth–dose against first HVT for a 10 cm × 10 cm field at 60 cm SSD at 1, 6 and 10 cm depth. For a given HVT at depths of 1–2 cm, any dependence of percentage depth–dose on peak tube potential is obscured by experimental uncertainties. However, such dependence becomes increasingly apparent as the depth is increased. For comparison, the broken curves show the data of *Br. J. Radiol. Suppl.* 11 which have been converted from 30 to 60 cm SSD using the method advocated by Burns (1958, and in BJR 1972 pp 101–3). Good agreement is apparent for low filtrations (the low HVT portions of the curves) but considerable discrepancies occur at higher HVTs and filtrations, particularly at depths greater than 10 cm. Johns *et al* (1953) upon whose work the relevant tables of *Br. J. Radiol.* (1972) are largely based, used relatively high tube potentials and low filtrations to obtain a particular HVT and under these conditions good agreement with the present works exists. Their data (and therefore that contained in *Br. J. Radiol.*

Table 3. Percentage depth–doses: 1.0 mm Al HVT.

Depth (cm)	Field size (cm^2) 0	7×7	10×10	15×15	20×20	30×30
			60 kV$_p$ (H = 0.673)			
0	100	100	100	100	100	100
1	54.0	63.0	68.6	69.3	69.4	69.5
2	34.0	41.0	43.0	43.0	45.0	46.0
3	20.3	28.0	29.5	30.2	31.7	32.1
4	13.0	20.0	21.0	22.0	23.0	24.0
5	8.3	13.8	15.0	16.2	16.7	16.8
6	5.5	9.6	10.8	12.0	12.2	12.4
7	3.8	7.5	8.4	9.2	9.6	9.7
8	2.6	5.5	6.2	7.1	7.4	7.5
9	1.8	4.1	4.7	5.5	5.7	5.8
10	1.3	3.1	3.6	4.2	4.3	4.4
12	0.68	1.6	2.1	2.4	2.6	2.8
14	0.36	0.90	1.3	1.5	1.6	1.7
16	0.19	0.54	0.88	0.96	1.0	1.0
			75 kV$_p$ (H = 0.588)			
0	100	100	100	100	100	100
1	54.0	63.0	68.6	72.4	74.0	74.1
2	34.0	42.0	48.0	50.0	51.6	51.6
3	20.3	29.0	33.4	36.7	38.1	38.3
4	14.0	21.0	24.7	27.9	28.1	28.2
5	9.3	16.0	18.5	21.0	21.9	21.9
6	6.5	11.8	14.0	15.8	16.7	17.2
7	4.4	8.8	10.9	12.6	13.5	13.9
8	3.2	6.5	8.3	10.0	11.2	11.2
9	2.3	5.0	6.4	7.9	8.2	8.8
10	1.7	4.2	5.2	6.3	6.8	6.9
12	0.92	2.4	3.2	4.0	4.5	4.5
14	0.52	1.5	1.9	2.5	2.9	3.0
16	0.29	0.66	1.2	1.6	2.0	2.0

Suppl. 11) is not, however, accurately applicable to more heavily filtered beams, especially at depths greater than 5 cm.

The ratio of first to second HVT is sometimes cited as a coefficient (H) of spectral homogeneity. In this paper both first HVT and peak tube potential are used to specify beam quality although it has been proposed (Trout *et al* 1962a) that the first HVT together with H might provide a more complete specification. On the other hand, a criticism of the homogeneity coefficient has been made by Hale (1966) on the grounds that it is a slowly varying function of peak tube potential for a given total filtration. However, neither Trout *et al* nor Hale discusses the precision with which H can be measured. Smoothed values of H for the various combinations of peak tube potential and filtration are given in table 1 and are in agreement with Hale's data generally to within ±3%. If first HVT and peak tube potential specify beam quality, then for a given first HVT, a reasonable experimentally attainable precision of ±3 kV for peak tube potential yields a precision of ±2% for percentage depth–dose (at 10 cm depth, 30 cm × 30 cm field and first HVT of 2 mm Al). If, however, the first HVT and H are used

Table 4. Percentage depth–doses: 1.5 mm Al HVT.

Depth (cm)	Field size (cm^2) 0	7×7	10×10	15×15	20×20	30×30
	60 kV_p ($H=0.681$)					
0	100	100	100	100	100	100
1	64.0	74.2	75.8	77.5	77.8	77.9
2	41.0	53.0	55.0	57.4	57.5	57.6
3	26.5	37.8	40.8	42.0	42.4	43.1
4	17.5	27.3	30.0	31.5	33.2	33.6
5	11.8	20.0	22.5	24.1	24.5	24.7
6	7.9	14.7	16.9	18.4	18.9	19.8
7	5.6	10.9	12.7	14.2	15.0	15.8
8	3.9	8.1	9.6	11.0	11.8	12.6
9	2.9	6.1	7.4	8.6	9.3	10.1
10	2.1	4.6	5.7	6.7	7.5	8.1
12	1.15	2.6	3.5	4.1	4.6	5.4
14	0.66	1.5	2.1	2.5	2.9	3.6
16	0.40	0.86	1.3	1.5	1.8	2.4
	75 kV_p ($H=0.590$)					
0	100	100	100	100	100	100
1	64.0	74.2	76.5	78.2	79.3	80.0
2	41.0	53.0	56.0	59.0	59.9	60.6
3	26.5	38.8	41.5	44.9	46.2	47.2
4	18.3	28.3	31.5	34.7	36.0	36.2
5	12.6	21.4	24.0	26.9	28.0	28.7
6	9.0	16.0	18.3	20.9	22.0	22.7
7	6.4	12.1	14.2	16.6	17.8	18.6
8	4.7	9.2	11.0	13.2	14.4	15.2
9	3.4	7.2	8.6	10.5	11.5	12.5
10	2.5	5.6	6.7	8.4	9.1	10.2
12	1.4	3.3	4.0	5.3	6.1	6.9
14	0.83	2.0	2.4	3.4	4.0	4.7
16	0.50	1.2	1.5	2.2	2.6	3.2
	90 kV_p ($H=0.554$)					
0	100	100	100	100	100	100
1	64.0	74.2	78.8	79.2	80.1	80.2
2	41.0	53.7	58.4	61.0	61.1	61.2
3	26.5	39.2	43.8	47.0	47.5	48.3
4	18.5	29.7	33.7	36.9	37.8	37.8
5	13.0	22.6	26.0	29.1	30.0	30.7
6	9.5	17.7	20.0	23.0	23.9	25.2
7	6.8	13.2	15.8	18.6	19.7	20.7
8	5.0	10.1	12.5	15.0	16.4	17.0
9	3.7	7.9	9.9	12.2	13.0	14.1
10	2.8	6.3	7.9	10.0	10.6	11.7
12	1.6	3.8	5.0	6.7	7.2	8.2
14	1.0	2.4	3.2	4.5	4.9	5.8
16	0.62	1.5	2.0	3.0	3.3	4.1

Table 5. Percentage depth–doses: 2.0 mm Al HVT.

Depth	Field size (cm^2)						Field size (cm^2)					
(cm)	0	7×7	10×10	15×15	20×20	30×30	0	7×7	10×10	15×15	20×20	30×30
	60 kV_p ($H = 0.714$)						75 kV_p ($H = 0.608$)					
0	100	100	100	100	100	100	100	100	100	100	100	100
1	68.0	80.0	83.2	84.0	84.8	84.9	68.0	80.0	83.2	84.0	84.8	84.9
2	45.5	60.8	64.3	66.4	67.1	67.8	45.5	60.8	64.3	66.4	67.1	67.8
3	31.0	46.0	49.8	51.6	52.0	52.3	31.5	46.0	49.8	52.5	53.0	54.3
4	21.0	33.2	38.5	40.0	41.2	41.4	22.0	34.8	38.5	41.0	42.8	43.3
5	14.3	24.8	28.7	31.1	31.7	32.5	15.7	26.5	29.4	32.3	33.6	34.7
6	10.0	18.4	22.0	24.2	25.0	25.6	11.2	20.0	23.1	25.5	27.1	27.8
7	7.2	13.8	16.8	18.8	19.9	20.4	8.2	15.3	18.0	20.4	21.8	22.7
8	5.1	10.4	12.8	14.6	15.8	16.3	5.9	11.8	14.1	16.3	17.4	18.6
9	3.7	7.9	10.1	11.5	12.5	13.1	4.4	9.3	11.0	13.1	14.4	15.4
10	2.7	6.0	7.9	9.1	10.0	10.6	3.3	7.0	8.6	10.5	11.4	12.7
12	1.5	3.5	4.7	5.7	6.3	7.1	1.9	4.3	5.3	6.8	7.2	8.8
14	0.87	2.0	2.8	3.6	4.1	4.7	1.2	2.6	3.3	4.4	5.1	6.1
16	0.51	1.2	1.7	2.3	2.7	3.1	0.70	1.6	2.1	2.8	3.6	4.2
	90 kV_p ($H = 0.558$)						100 kV_p ($H = 0.538$)					
0	100	100	100	100	100	100	100	100	100	100	100	100
1	68.0	80.0	83.2	84.0	84.8	84.9	68.0	80.0	83.2	84.0	84.8	84.9
2	45.5	60.8	64.3	66.4	67.1	67.8	45.5	60.8	64.3	66.4	67.1	67.8
3	31.5	46.0	49.8	52.8	53.8	54.4	31.5	46.0	49.8	52.8	54.2	55.0
4	22.0	35.2	38.5	42.0	43.2	44.3	22.0	35.2	38.5	42.9	44.0	45.0
5	15.7	27.0	31.0	34.0	34.8	36.5	16.0	27.4	31.1	34.8	36.1	37.5
6	11.2	20.9	24.5	27.5	28.2	30.0	11.4	21.7	24.5	28.2	29.7	31.2
7	8.2	16.2	19.5	22.2	23.2	25.1	8.5	16.8	19.8	23.0	24.6	26.1
8	5.9	12.6	15.5	18.0	19.2	21.0	6.3	13.0	16.0	18.8	20.4	21.9
9	4.4	9.8	12.5	14.7	15.7	17.4	4.7	10.5	13.0	15.5	16.5	18.5
10	3.3	7.6	10.1	12.0	12.7	14.5	3.5	8.3	10.5	12.7	13.8	15.7
12	1.9	4.8	6.4	8.0	8.8	10.3	2.0	5.3	6.9	8.6	9.5	11.3
14	1.2	3.0	4.1	5.4	6.0	7.3	1.2	3.4	4.5	5.8	6.8	8.2
16	0.70	1.9	2.6	3.6	4.1	5.2	0.78	2.2	2.9	3.9	4.9	6.0

Table 6. Percentage depth–doses: 3.0 mm Al HVT.

Depth (cm)	Field size (cm²) 0	7×7	10×10	15×15	20×20	30×30
			75 kV$_p$ ($H = 0.755$)			
0	100	100	100	100	100	100
1	73.5	87.7	90.4	91.8	92.1	92.5
2	52.0	70.7	74.2	76.0	77.0	77.7
3	37.0	55.2	59.5	62.7	63.7	64.6
4	27.0	43.0	46.4	51.2	52.6	53.0
5	19.0	33.5	37.5	41.4	43.8	44.0
6	14.0	26.4	30.3	33.4	35.7	36.6
7	10.0	20.7	24.0	26.9	29.0	30.1
8	7.5	16.0	19.0	21.6	23.0	24.8
9	5.6	12.4	15.1	17.6	19.0	20.7
10	4.2	9.8	12.0	14.3	15.4	17.2
12	2.5	6.1	7.7	9.4	10.4	12.0
14	1.5	3.8	4.9	6.1	6.9	8.4
16	0.93	2.3	3.1	4.3	4.5	5.9
			90 kV$_p$ ($H = 0.657$)			
0	100	100	100	100	100	100
1	73.5	87.7	90.4	91.8	92.1	92.5
2	52.0	70.7	74.2	76.0	77.0	77.7
3	37.0	55.2	59.5	62.7	63.7	64.6
4	27.5	43.0	47.4	51.2	52.6	53.7
5	20.0	34.0	38.1	42.2	44.0	44.8
6	14.5	26.6	30.7	34.7	35.7	37.4
7	11.0	20.9	24.5	28.3	29.5	31.5
8	8.1	16.5	19.6	23.0	24.3	26.6
9	6.2	13.0	15.7	19.0	20.1	22.3
10	4.7	10.2	12.6	15.5	16.5	18.7
12	2.8	6.5	8.3	10.5	11.5	13.5
14	1.7	4.1	5.5	7.1	8.2	9.7
16	1.1	2.6	3.6	5.3	5.8	7.0
			100 kV$_p$ ($H = 0.590$)			
0	100	100	100	100	100	100
1	73.5	87.7	90.4	91.8	92.1	92.5
2	52.0	70.7	74.2	76.0	77.0	77.7
3	37.0	55.2	59.5	62.7	63.7	64.6
4	27.5	43.0	48.0	52.0	52.6	55.0
5	20.5	34.5	38.9	43.0	44.2	46.3
6	15.2	27.0	31.6	35.6	37.1	39.0
7	11.3	21.7	25.5	29.4	31.0	33.0
8	8.7	17.4	20.5	24.3	25.7	28.0
9	6.7	13.7	16.8	20.1	21.5	23.9
10	5.0	10.9	13.7	16.7	17.8	20.4
12	3.1	7.0	9.0	11.6	12.5	14.8
14	1.9	4.5	5.9	8.0	8.8	10.7
16	1.2	2.9	3.9	5.5	6.2	7.7

Table 7. Percentage depth–doses: 4.0 mm Al HVT.

Depth (cm)	Field size (cm²) 0	7×7	10×10	15×15	20×20	30×30
			100 kV$_p$ ($H=0.704$)			
0	100	100	100	100	100	100
1	76.0	90.6	93.6	94.2	95.0	96.8
2	55.0	75.0	80.2	81.3	83.6	86.0
3	40.5	60.6	66.4	69.5	72.9	73.4
4	30.5	48.5	54.3	58.4	60.5	63.2
5	23.0	38.5	44.5	48.9	51.7	53.9
6	17.0	30.8	36.5	41.0	43.6	46.0
7	13.0	25.2	29.8	34.1	36.6	39.1
8	10.1	20.5	24.3	28.4	30.5	33.2
9	7.7	16.3	19.9	23.7	26.0	28.6
10	5.7	13.1	16.3	19.8	21.6	24.7
12	3.5	8.4	10.8	13.9	15.2	17.9
14	2.2	5.3	7.2	9.7	10.6	13.0
16	1.4	3.4	4.8	6.8	7.2	9.4

to specify quality, then an attainable precision of ±3% for H yields a ±4% precision for the percentage depth–dose.

Thus the first HVT together with either peak tube potential or homogeneity coefficient can provide alternative specifications of beam quality. The use of peak tube

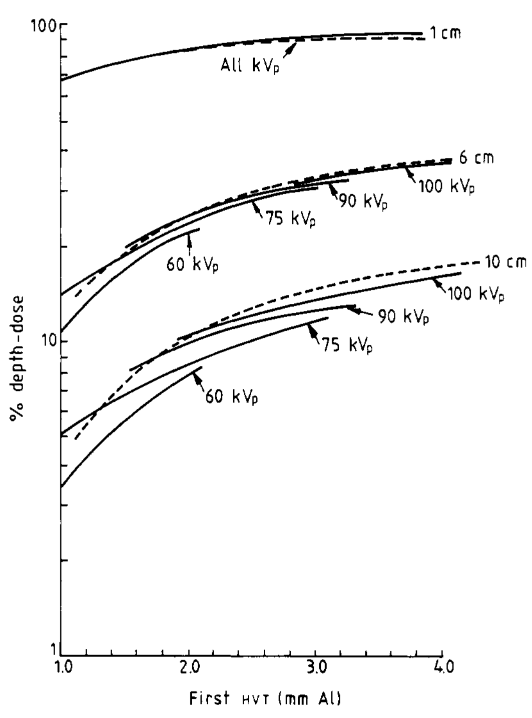

Figure 1. Percentage depth–dose against first HVT for a 10 cm × 10 cm field at 60 cm SSD at 1, 6 and 10 cm depth. The full curves are experimental data and broken curves refer to the data of *Br. J. Radiol. Suppl.* 11 converted to 60 cm SSD.

potential may be preferred in practice since a sufficiently accurate value is usually known or can easily be measured with a calibrated penetrameter, whereas a measurement of the homogeneity coefficient is more time-consuming. However, values of H for each combination of first HVT and peak tube potential are given in tables 3–7 and may be used if preferred.

In comparing the present depth-dose measurements with those of *Br. J. Radiol. Suppl.* 11, use has been made of the formula cited by Burns (pp 101–3) for conversion of data from one SSD to another, namely

$$P(d, f_2, S_0) = P(d, f_1, S_0/F)(B(S_0/F)/B(S_0))F^2 \quad (1)$$

where

$$F = [(f_1 + d)/f_1][f_2/(f_2 + d)]$$

and P = percentage depth–dose at depth d, SSD = f, and field size at the surface = S_0. Also f_1 is the known SSD, f_2 the new SSD and B is the backscatter factor. Burns states that this expression agrees with experimental data to within ±2% over the first HVT range 2 mm Al to 4 mm Cu. A comparison of depth doses for 10 cm × 10 cm and 30 cm × 30 cm fields at 1.14 mm Al HVT at SSDs of 60 and 100 cm confirmed the validity of equation (1) within the limits of experimental error. Percentage depth–doses at 10 cm depth for 60 cm SSD would change by not more than ±10% upon conversion to SSDs within the range 45–90 cm.

Theoretical zero-area data derived from calculated spectra are plotted against HVT for 1, 2, 6 and 10 cm depth in figure 2. Similar families of curves for each depth are seen corresponding to the use of different peak tube potentials as observed in the large-field depth–dose measurements. In general, the model indicates that for a given first HVT, a higher peak tube potential gives a higher percentage depth–dose, but at 1 cm depth this trend is reversed, as expected. The small differences, at 1 cm depth, between theoretical percentage depth–doses for the range of tube potentials considered were not observed experimentally and therefore for a given first HVT no distinction was made between the various values of tube potential when tabulating PDDs at small depths. Experimental zero-area percentage depth–doses are generally not more than 10% higher than the theoretical values and this difference becomes smaller with increasing depth. Figure 3 shows theoretical and experimental zero-area data at depths of 1 and 10 cm together with the corresponding data from *Br. J. Radiol. Suppl.* 11, converted to 60 cm SSD. The latter data are in good agreement with the present experimental work and with theory at depths >6 cm, but significant differences arise at smaller depths. The zero-area depth–doses in tables 3–7 refer to the experimental data.

7. Comparison with other work

Other compilations of depth–dose data for the diagnostic range (in addition to those taken into account in the preparation of *Br. J. Radiol. Suppl.* 11) include those of Seelentag and Klotz (1959) and Trout *et al* (1952, 1962b). These data are presented in graphical rather than in tabulated form. The uncertainties associated with reading and interpolating the data allow only rough comparisons with the present work to be made.

Seelentag and Klotz measured depth–dose data for 150 cm^2 fields at 35 cm SSD. Conversion to 60 cm SSD and comparison of data at the same HVT and tube potential indicates agreement to within ±10%.

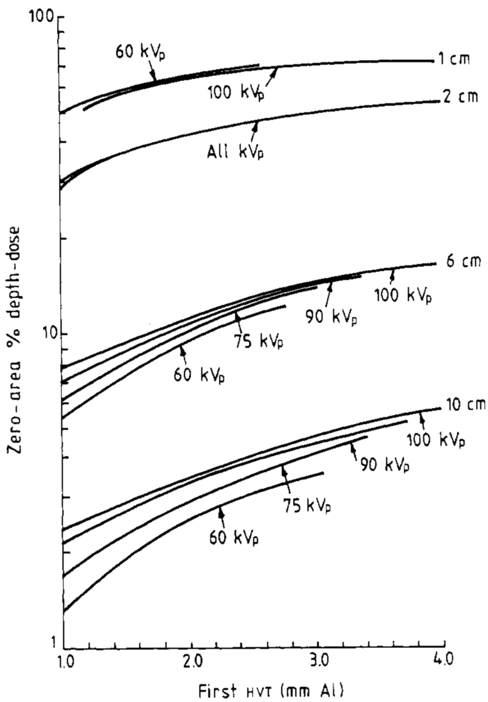

Figure 2. Theoretical zero-area percentage depth–dose against first HVT for 1, 2, 6 and 10 cm depth and 60 cm SSD.

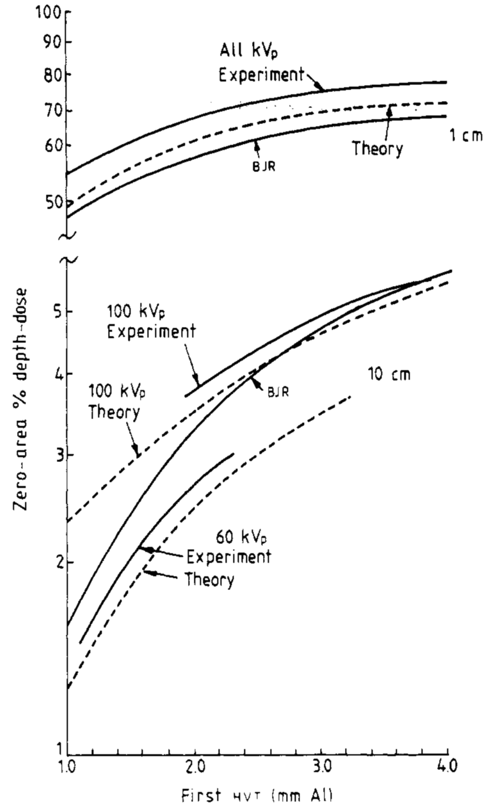

Figure 3. Theoretical and experimental zero-area percentage depth–dose against first HVT for 1 and 10 cm depth at 60 cm SSD. The data of *Br. J.Radiol. Suppl.* 11, converted to 60 cm SSD, is also given for comparison (labelled BJR).

Trout *et al* (1952) have published measurements for two field sizes, 8 inch × 10 inch (516.6 cm^2) and 14 inch × 17 inch (1538 cm^2) using a Victoreen thimble chamber. For all beam qualities, the percentage depth–doses are significantly higher (up to 20%) than the measurements reported here. This may be due to the unsuitable characteristics of the thimble chamber for measurement in a phantom as discussed by Adams (1962) combined with chamber size effects discussed previously.

Further work by Trout *et al* (1962b) using a different ionisation chamber indicates agreement with the present measured data to within ±10% for an 8 inch × 10 inch field at 100 kV$_p$ for HVTs of 1.7 and 3.4 mm Al.

Acknowledgments

I would like to thank Dr M J Day for his encouragement and advice on many aspects of this work and helpful criticism during the preparation of the manuscript. I am grateful to Mr R Birch for kindly supplying a copy of a computer program for calculating theoretical x-ray beam spectra.

Résumé

Dose en profondeur le long de l'axe central en radiologie diagnostique.

La dose en profondeur a été mesurée pour différentes conditions d'irradiation en radiologie diagnostique, afin de fournir des bases pour le calcul de dose au malade, provenant de plusieurs explorations radiologiques. En général, nous avons besoin de données correspondant à des champs plus grands, des distances sources-objets plus longues et des filtres plus épais que ce que l'on trouve en radiothérapie. On discute les principes et les techniques de mesure, en s'attachant particulièrement à la qualité du faisceau de rayons X. On recommande que la tension maximale du tube et la valeur de la première couche de demi-atténuation soient spécifiées en particulier pour la détermination des doses à une profondeur de 5 cm ou plus. Avec la qualité du faisceau requise, ces mesures s'accordent bien avec les autres ensembles de données utilisées en radiothérapie. On a mesuré les doses en profondeur sur une surface nulle et on les a comparé aux valeurs calculées obtenues à partir des considérations théoriques sur le spectre de rayons X.

Zusammenfassung

Tiefendosiswerte entlang der Zentralachse für die Röntgendiagnostik.

Für einen großen Bereich von Bestrahlungsbedingungen, die für die Röntgendiagnostik relevant sind, wurden Tiefendosiswerte gemessen als Basis zur Berechnung der Patientendosierung bei Röntgenuntersuchungen. Im allgemeinen sind hier Daten für größere Felder, größere Quellen-Oberflächen-Abstände und größere Röhrenfilterungen erforderlich als normalerweise in der Strahlentherapie. Meßprizipien und Techniken werden diskutiert unter Berücksichtigung der Spezifizierung der Röntgenstrahlqualität. Dabei sollten sowohl die maximale Röhrenspannung wie auch die erste Halbwertsdicke angegeben werden, vor allen Dingen zur Bestimmung der Dosis in einer Tiefe von 5 cm und mehr. Mit der dazugehörigen Spezifizierung der Qualität wurde eine gute Übereinstimmung zwischen diesen Messungen und anderen Zusammenstellungen von Tiefendosiswerten für die Strahlentherapie gefunden. Außerdem wurden die Tiefendosen bei Feldfläche Null gemessen und verglichen mit berechneten Werten, die man aus theoretischen Überlegungen von Röntgenstrahlspektren erhält.

References

Adams G D 1962 *Radiology* **78** 77–89

Birch R and Marshall M 1979 *Phys. Med. Biol.* **24** 505–17

Birch R, Marshall M and Ardran G M 1979 *Catalogue of Spectral Data for Diagnostic X-rays* SRS 30 (HPA, 47 Belgrave Square, London SW1X 8QX)

Burns J E 1958 *Br. J. Radiol.* **31** 643

BJR 1972 *Central Axis Depth Dose Data for use in Radiotherapy Br. J. Radiol.* Suppl 11

Code of Practice for the Protection of Persons against Ionizing Radiations arising from Medical and Dental use 1972 (London: HMSO)

Epp E R and Weiss H 1967 *Radiat. Res.* **30** 129–39

Greening J R 1963 *Br. J. Radiol.* **36** 363–71

Hale J 1966 *Radiology* **86** 147–8

HPA 1977 *The Physics of Radiodiagnosis* SRS 6 (HPA, 47 Belgrave Square, London SW1X 8QX) p 56

ICRU 1970 *Radiation Dosimetry: X-rays Generated at Potentials of 5–150 kV* Report 17 (ICRU Publications, PO Box 30165, Washington, DC 20014, USA)

—— 1973 *Measurement of Absorbed Dose in a Phantom Irradiated by Single Beam of X or Gamma Rays* Report 23 (ICRU Publications, PO Box 30165, Washington, DC 20014, USA)

Johns H E, Epp E R and Fedoruk S O 1953 *Br. J. Radiol.* **36** 32–7

Seelentag W and Klotz E 1959 *Strahlentherapie* **108** 112–26

Trout E D, Kelly J P and Cathey G A 1952 *Am. J. Roentgenol.* **67** 946–63

Trout E D, Kelly J P and Lucas A C 1960 *Am. J. Roentgenol.* **84** 729–40

—— 1962a *Am. J. Roentgenol.* **87** 574–84

—— 1962b in *Technological Needs for Reduction of Patient Dosage from Diagnostic Radiology* (Springfield IL: C C Thomas)